

## ANALYSIS OF MACROSCOPIC FRACTURES IN THE CAJON PASS SCIENTIFIC DRILLHOLE: OVER THE INTERVAL 1829 - 2115 METERS

Colleen A. Barton and Daniel Moos

Department of Geophysics, Stanford University, California

**Abstract.** The orientation, distribution and apparent aperture of natural fractures intersecting the Cajon Pass research well were determined through analysis of borehole televiewer (BHTV) data over the interval 1829 to 2115 meters. Large open fractures have shallow inclinations and tend to be aligned striking roughly N15°E. There is no apparent relationship between these fractures and the current stress state, as measured by the analysis of wellbore breakouts and hydraulic fracturing experiments in the Cajon Pass well and as observed in other studies in the region. Temperature anomalies due to fluid flow into the well detected during a long-term permeability experiment occur at several of these fractures. Compressional, shear and Stoneley guided wave velocities are within the expected range for crystalline rocks and elastic-wave anomalies are associated with the larger fractures. Stoneley wave coherence is reduced where the fractures are hydraulically conductive.

## Introduction

The properties of crystalline rock masses are profoundly affected by the presence of fractures. Permeability [e.g. Brace, 1980], seismic velocities [e.g. Stierman and Kovach, 1979] and seismic anisotropy [Crampin et al., 1980] are often controlled by fracturing. Fractures provide permeable pathways for fluids which further affect rock properties by chemical alteration of the surrounding rock mass. The relative importance of fractures in controlling rock properties depends on the fracture density and orientation, as well as the hydraulic and mechanical characteristics of the fractures themselves.

The Cajon Pass research well reached a total depth of 2115 m at the end of the first phase of experimentation. The borehole diameter above 1829 m is significantly larger than the 30.5 cm bit size resulting in lower quality BHTV data in the uppermost section of the borehole. Data collected in the interval from 1829 to 2115 m is of excellent quality, however, and revealed numerous zones of wellbore spalling [Shamir et al., this issue] as well as a number of fractures intersecting the borehole. Full waveform sonic logs were recorded over this interval, from which compressional, shear and Stoneley wave velocities were calculated. A long-term permeability study was carried out to measure the transmissivity of the open-hole interval [Coyle and Zoback, this issue] and continuous temperature [Lachenbruch and Sass, this issue] and fluid conductivity [Kharaka, this issue] logs were also obtained while fluid was flowing into the borehole. The combined data provides a unique opportunity to study fracture orientations and properties near the San Andreas fault.

## BHTV Data Acquisition

The borehole televiewer is an ultrasonic well logging tool useful for measuring the orientation and distribution of fractures and stress-induced wellbore breakouts and for examining lithostratigraphic features. The analog televiewer [Zemanek, et al., 1970] contains a transducer that emits a

focused 3° beam, 1.4 MHz acoustic pulse at a rate of 1800 per second. The transducer rotates three revolutions per second as the tool moves vertically up the borehole at a speed of 2.5 cm/s. Ultrasonic seismograms are transmitted through a standard wireline logging cable and recorded on videotape. A fluxgate magnetometer within the tool makes it possible to orient the data with respect to magnetic north.

The analog waveforms are windowed around the reflected pulse from the borehole wall and digitized at 1 μs intervals [Barton, 1988]. This results in the dual measurement of the acoustic reflectivity of the borehole wall and the ultrasonic travel time of the imaging pulse at a spatial resolution well above conventional logging tools. The resolution of the televiewer is a function of the borehole size, logging speed and the tool geometry.

## Fracture Analysis from BHTV Images

Digital BHTV data acquired in the Cajon Pass well from 2114 m to 1829 m were analyzed to determine the characteristics of natural fractures intersecting the drillhole. The data were median filtered before analysis to eliminate noise spikes that arise during the analog to digital conversion and from anomalous multiple arrivals. In this study we have discriminated between planar features according to apparent width, that is, the gap measured by the televiewer, across a planar fracture as it intersects the borehole. A variety of factors including the mechanical erosion of the fracture surface and the geometry of the acoustic reflection of the BHTV signal, which is controlled by the transducer beam width and the size of the feature, preclude the measurement of true fracture aperture away from the borehole.

Fracture distribution and qualitative size were determined through the analysis of cylindrical wire frame projections of the data to a scale which preserves the correct aspect ratio. This reconstruction of the topography of the borehole emphasizes fine scale features that may not be visible on conventional displays of reflectivity or borehole radius. It also aids in discriminating between two or more intersecting fractures and isolating fractures from other borehole features such as breakouts.

Planar features were grouped by apparent aperture into three categories. The apparent width is the minimum fracture width observed in cross sections of the fracture plane where correction for the apparent dip of the fracture has been made. Many fine scale features are interpreted as foliation based on their similarity to low angle, fine scale features visible in core. Larger features may be fracture zones or faults that have been in-filled with debris. A total of 365 features were identified from the BHTV images and are combined to show the fracture density per meter in the second profile of Figure 1. Aside from the interval from 1940 to 1960 m of stress-induced wellbore breakouts [Shamir et al., this issue], which contain only a few observable fractures, the fracture population shows no trend in size or distribution with depth over the logged interval. These results are in contrast with a fracture analysis from an Illinois drillhole where fracture density and hydraulic conductivity decrease with depth [Haimson and Doe, 1983]. Fracture studies of ten wells located in the western Mojave Desert just west of the Cajon Pass well by Seeburger and Zoback [1982] found only a slight decrease of fracture density with depth for most wells studied. They found some wells to have a uniform

Copyright 1988 by the American Geophysical Union.

Paper number 8L7348.  
0094-8276/88/008L-7348\$03.00

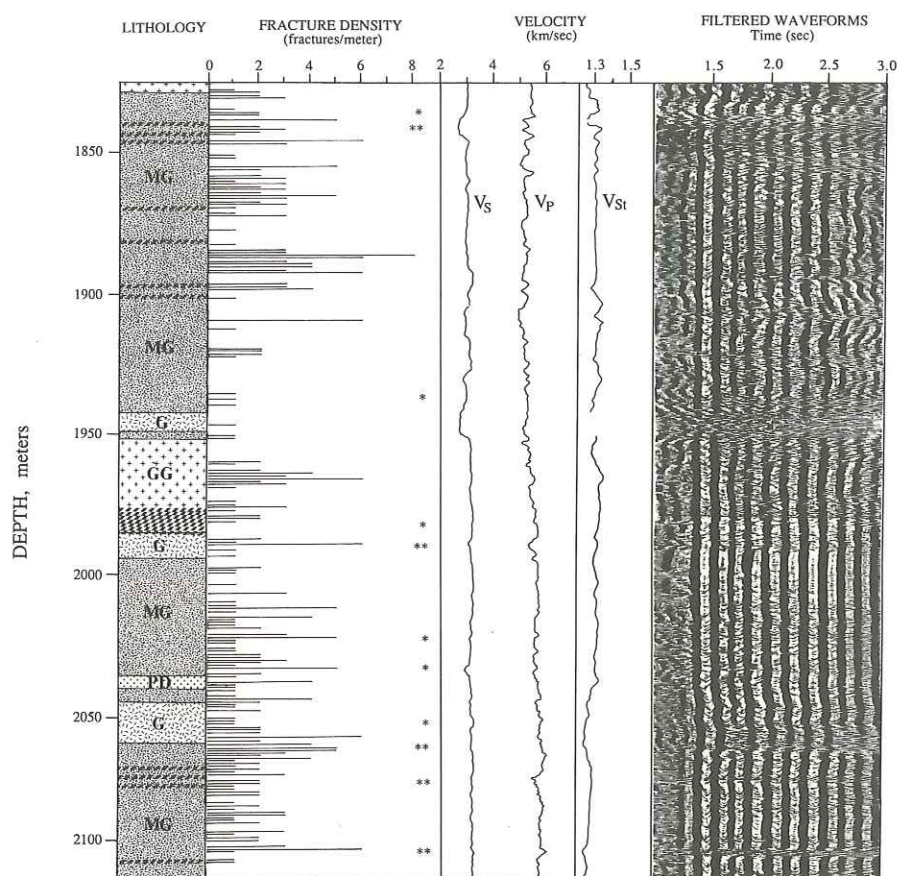


Fig. 1. Lithology, fracture density, sonic velocities and filtered waveforms over the interval 1829 to 2115 in the Cajon Pass research well. A simple count of fracture density is poorly correlated with the sonic arrival times displayed on the right. By weighting the fractures by their apparent aperture (asterisks), a much stronger correlation is observed.

fracture density distribution while others showed concentrations of fractures at various depths as is the case in the Cajon Pass well. Figure 1 also shows the comparison of fracture distribution to lithology in the Cajon Pass well [after Silver, unpublished data]. The relationship between lithology and fracturing is discussed below.

The apparent width of a fracture in BHTV images is probably larger than its true aperture. The rock surrounding a fracture may be weaker due to chemical alteration and preferentially broken by the destructive drilling process. It is likely then that the aperture of a fracture at the intersection of the borehole is greater than its aperture away from the borehole. Repeated pipe trips into and out of the hole and fluid circulation further increase the apparent fracture width at the borehole wall.

Figure 2a shows cross-sections for a fracture at 2076 m where the plane of the fracture has been determined and the cross-sectional profiles are corrected for apparent dip of the fracture. These sections were constructed at azimuth intervals of  $60^\circ$  around the borehole. Many fractures imaged by the BHTV do not have abrupt breaks at their boundary with the intact rock — instead, that boundary is often sloped in cross-section (c.f. Figure 2a  $90^\circ$  profile). Detailed cross-sections through the fracture image can be used to measure its minimum apparent width. Through the evaluation of several fracture cross sections an average apparent fracture width is determined. Figure 2b shows cross sections over about 0.75 meters of smaller aperture fractures at depth 1995 m.

Where fractures are open along the extent of their intersection with the borehole to the resolution of the BHTV imaging apparent fracture aperture could be measured. The

double asterisks in the second profile of Figure 1 correspond to zones where the fracture width per meter is greater than 10 cm; the single asterisks to zones with fracture width between 5 and 10 cm. The remaining intervals have nominal apparent aperture per meter. In several intervals with a high frequency of fractures the cumulative width per meter is quite low. However, where the apparent aperture per meter is large there are usually a large number of fractures. Although mechanisms acting to close fractures would be expected to reduce the number of open fractures with increasing depth, the data do not show this trend.

Only those through-going planar features that are open to an apparent width greater than 1 cm can be analyzed for

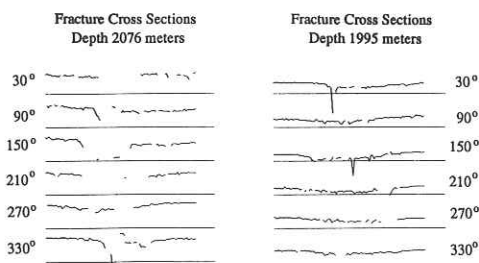


Fig. 2. a) Cross sections across fracture at 2076 m where apparent aperture is about 26 cm. Sections are constructed at azimuth spacings of  $60^\circ$  and are corrected for apparent dip. b) Cross sections across a 0.75 m fracture zone at 1995 m where individual fractures are less than 5 cm.

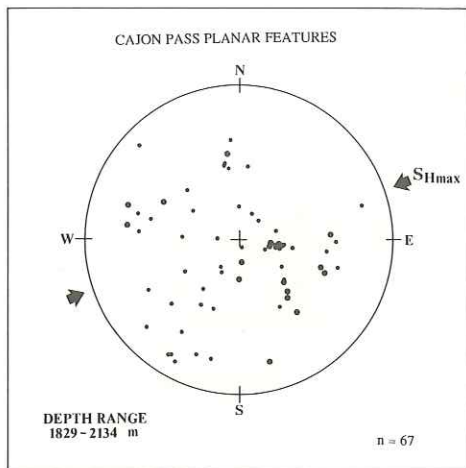


Fig. 3. Lower hemisphere equal area projections of the poles to fracture surfaces in the interval 1829 to 2115 m in the Cajon Pass research well. Large fractures are shown as larger symbols. Although the smaller features have random orientations, a cluster of large fractures is present striking N15E, dipping approximately  $30^\circ$  west northwest.

orientation, substantially reducing the number of fractures where orientation can be determined. Fractures that intersect the borehole appear as sinusoids on unwrapped  $360^\circ$  views of reflectivity and borehole diameter. These sinusoids are often discontinuous for fine scale fractures and they can show very complex patterns at points where several fractures intersect or where fractures are not perfectly planar. For this reason automatic curve fitting routines cannot be used and interactive graphics are required to fit the sinusoidal shapes [Barton, 1988]. To measure fracture orientation the amplitude and phase of a best fit sinusoidal shape to the fracture are found using a graphics mouse with the standard  $360^\circ$  display of the image. The dip angle of the fracture plane is then the inverse tangent of the ratio of the fracture height to the borehole diameter. The dip direction is the direction of the lowest point on the sinusoid, and the strike is  $90^\circ$  to the dip direction.

Fracture orientations are shown in the Schmidt diagram in Figure 3. Small circles represent the poles of fractures with apparent widths between 1 and 5 cm, and large circles the poles of fractures over 5 cm. Although there is substantial scatter in fractures orientations the majority of large fractures strike north northeast, with moderately shallow dips to the northwest. No trend in fracture orientation was observed with depth.

The orientation of maximum horizontal principal stress at the Cajon Pass site is  $73^\circ$  based on breakout data [Shamir et al., this volume], and hydraulic fracturing experiments [Zoback and Healy, this volume]. Stress magnitude measurements indicate a normal faulting stress regime at shallow depth in the Cajon Pass well. Fractures developed under this ambient stress field would be expected to have east northeast orientations. Thus, there appears to be no obvious relationship between the orientations of fractures over the interval 1829 to 2115 m and the current stress field. There is no evidence that Mode I extension [see Engelder, 1982] prevails at this depth nor are these fractures easily interpreted as shear features.

#### Correlation of Natural Fractures with Other Data

Core analysis over this interval was completed by Silver and James [unpublished data] and the simplified lithology is shown in Figure 1. The major units are mafic granite (MG), granitic gneiss (GG), and younger intrusions of granite (G). The diagonal symbol represents zones of migmatites or highly foliated rock. A pegmatite dike (PD) intersects the well at 2040

m. Over the interval 1850 to 1950 m the mafic granite includes several migmatite zones which appear to separate alternating intervals of high and low fracture frequency. The interval 1940 to 1960 m corresponds to a zone of extremely wide breakouts; it is not possible to determine if the low density of fractures over this interval is real or a function of the image quality. Below 2000 m there is uniform fracture distribution although the interval includes several migmatite zones. From 1950 to 2000 m the gneissic granite and overlying and underlying migmatites have a relatively high fracture density with very low measurable aperture. This relationship is attributed to the abundant measurement of foliation planes in the BHTV analysis.

At the time of this analysis comprehensive geophysical logs were not available, however, the Cajon Pass experiment has provided an ideal set of complementary data for the analysis of the acoustic waveform response to fluid filled fractures. The complete BHTV log and the digital analysis of fracture geometry were used in conjunction with the full waveform sonic data to determine the response to fractures. The third and fourth profiles in Figure 1 shows the computed compressional, shear, and Stoneley wave velocities and the filtered waveforms for the interval 1829 to 2115 m in the Cajon Pass well. Note that there is little apparent relationship between fracture density and sonic velocities. A much greater correlation exists between the velocities and the cumulative apparent aperture per meter determined from the BHTV logs. Velocities are relatively constant over this interval ( $V_p$  5.5 to 6.0;  $V_s$  3.0 to 3.3 km/s).  $V_p/V_s$  is about 1.75. Several low velocity zones occur at 1835-1845 m, 1940-1960 m ( $V_s$  only), and at 1995, 2026, and 2076 m. Stoneley velocities are about 1.3 km/s in the 26 cm borehole above 2045 m, and 1.25 km/s in the 20 cm borehole below. Low waveform coherence occurs at 1840, 2026, 2045, 2065, 2076 and 2102 m, and 1940-1960 m. Some of these depths are associated with lower Stoneley velocities. Each of the intervals listed above contains fractures with measurable apertures, ranging from more than 25 cm (2102 m) to somewhat less than 10 cm (2026 m).

Data from a series of precision temperature logs [Lachenbruch, this volume], an electrical conductivity log of the borehole fluid [Kharaka, this volume] and measurements of the concentration of fluorescene dye used to tag the drilling fluid before initiation of a fluid drawdown test can be used to determine the origin of the fluid being drawn into the well. Fluid flowing into the well within a narrow zone will offset the temperature profile, giving an anomalously low thermal gradient at the fracture. For example, the gradient minimum at 2076 m correlates with a major fracture observed in the BHTV image which has a measured aperture of 26.6 cm (Figure 2a). This fracture correlates exactly with a change in fluid conductivity gradient [Kharaka, this volume] and a drilling break where the penetration speed of the drill bit was suddenly accelerated [Silver, written comm.]. Fluorescene concentrations in fluids below 2076 m are equal to those of the original drill fluid, implying no influx of formation water below that depth. The fracture series at 1995 m (Figure 2b) has a cumulative aperture of 20.9 cm over 1 m, but no associated temperature anomaly. Additional fractures delineated in the BHTV log that also correlate with minima in the thermal gradient occur at 1840, 1940, 2026, and 2065 m. Thus many of the large natural fractures that intersect the Cajon Pass drillhole have an expression in the temperature logs, suggesting that they are hydraulically conductive and have supplied fluid during the drawdown recovery. Fractures with apparent apertures less than about 5 cm do not appear to have significant hydraulic conductivity.

Table I presents the results of fracture aperture and sonic wave analyses of all of the major features observed in the Cajon Pass well from 1829 to 2115 m. Also shown are the other anomalies associated with these fractures. Anomalies not associated with fractures (such as those due to the change in hole size at 2046 m) are not shown. Note that all of the

Table 1. CAJON PASS FRACTURE COMPARISON

DEPTH meters	Fracture Aperture	Stoneley Wave	Refracted Waves	Fluid ** Conductivity	Drilling Break	Temperature
1841	13.5	v/c	v/c	X	X	X
1940	4.6	***	***	X		X
1995	20.9		v/c			
2026	11.7	c	v	X?	X	X*
2065	31.8	c	c			X
2076	26.6	c	v/c	X		X
2102	34.3	v/c	c	-	X	?

v=velocity change

c=coherence change

\* Temperature anomaly appears on 5/14 temperature profile only (Lachenbruch and Sass, this volume)

\*\* Depths are approximate (Y. Kharaka, this volume)

\*\*\* Elastic properties obscured by severe breakouts

fractures with Stoneley anomalies also have thermal gradient minima, except that at 2102 m; the possible presence of a Stoneley anomaly is obscured for the fracture within the breakouts at 1940 [see Shamir, et al., this volume]. Drilling breaks were seen at three fractures. All of the fractures had some anomalous refracted (P and S) wave response, although again the lack of response at 1940 m may be due to the breakouts.

Previous research has demonstrated a relationship between Stoneley wave amplitude and permeability [Paillet, 1980; Burnes, et al., 1988]. Here, we see a reduction in Stoneley wave coherence at fractures which by other indications appear to be permeable. This is not unreasonable as the mechanism proposed for Stoneley wave amplitude reduction (scattering, reflections, etc.) would also reduce coherence. The relationship between Stoneley wave coherence and fractures is generally supported by these data, except for the interval 1992-1996 m. A cross section across this fracture zone was presented in Figure 2b where a series of thin parallel fractures span approximately 0.75 m in the borehole. Compressional and shear velocities are lower within the fractured interval, but  $V_p/V_s$  is unchanged. The waveforms are distorted due to the reduced coherence of the arrivals, although the Stoneley wave arrival is unaffected. For the large fracture at 2076 m the Stoneley wave is strongly attenuated. The refracted arrivals are also less coherent, although in this case the velocities are unchanged. Both temperature and fluid conductivity are affected at this depth. The aperture of the fracture at 2076 m is 26.6 cm, only slightly greater than the 20.9 cm cumulative aperture over the fracture zone at 1995 m. Although the zone at 1995 m shows no evidence of hydraulic conductivity, the velocities and coherence of refracted waves are lower, suggesting that these fractures are mechanically weak.

The data shown in Table I indicate that the fracture at 2076 m is not the only permeable fracture. However, not all of the measurably open fractures contribute to the total permeability. Based on the Stoneley response the most conductive fractures are at 1840 and 2076 m. One inconsistency in these data is the apparently high permeability of the fracture at 2102 m which, based on the constant fluorescence concentration below 2076 m, has not contributed any fluid. The only explanation of these observations is that this fracture has no connectivity to a fluid source.

### Conclusions

More than 300 planar features have been observed in borehole televiewer data over the interval 1829 to 2115 m in the Cajon Pass well. Most of these are probably foliation planes. Only 67 through-going features were identified and measured for orientation. Based on their orientation, the larger fractures are not associated with the current stress field. The relationship between fracturing and sonic velocities is clearer if the apparent fracture aperture rather than simply the density of natural fractures, is used. Indications of enhanced

permeability are associated with many of the larger features. These are also characterized by reductions in Stoneley wave coherence, in agreement with theoretical studies.

**Acknowledgements.** The authors would like to thank the reviewers for their recommendations during the preparation of this manuscript. Funding was provided by the Continental Lithosphere Program of the National Science Foundation through DOSECC and by the contributors to the Stanford Rock Physics and Borehole Geophysics Project.

### References

- Barton, C.A., Development of in-situ stress measurement techniques for deep drillholes, Ph.D. Thesis Stanford University, Department of Geophysics, 1988.
- Brace, W.F., Permeability of crystalline and argillaceous rocks, *Int. J. Rock Mech. Min. Sci. & Geomech. Abstr.*, **17**, 241-251, 1980.
- Burnes, D.R., Cheng, C.H., Schmitt, D.P. and Toksoz, M.N., Permeability estimation from full waveform acoustic logging data, *The Log Analyst*, **29**, 112-122, 1988.
- Crampin, S., McGonie, R. and Bamford D., Estimating crack parameters from observations of P-wave velocity anisotropy, *Geophysics*, **45**, 345-360, 1980.
- Engelder, T., Is there a genetic relationship between selected regional joints and contemporary stress within the lithosphere of North America?, *Tectonophysics*, **1**, 161-177, 1982.
- Haimson, B. C. and Doe, T.W., State of stress, permeability and fractures in the Precambrian granite of northern Illinois, *Journ. Geophys. Res.*, **88**, 7355-7371, 1983.
- Paillet, F. L. Acoustic propagation in the vicinity of fractures which intersect a fluid filled borehole, *SPWLA 21st Ann. Log. Symp. Paper D*, 1980.
- Seeberger, D.A. and Zoback, M.D., The distribution of natural fractures and joints at depth in crystalline rock, *Journ. Geophys. Res.*, **87**, 5517-5534, 1982.
- Stierman, D.J. and Kovach R. L., Pressure induced velocity gradient: an alternative to a Pg refractor in the Gabilan Range, central California, *Bull. Seis. Soc. Am.*, **69**, 397-415, 1979.
- Zemanek, J., Glenn, E.E., Norton, L.J. and Caldwell, R.L., Formation evaluation by inspection with the borehole televiewer, *Geophysics*, **35**, 254-269, 1970.

C.A. Barton and D. Moos, Stanford University,  
Department of Geophysics, Stanford, CA 94305.

(Received: March 17, 1988;  
revised: June 17, 1988;  
accepted: June 17, 1988.)